

Pattern of Expression of p53, Its Family Members, and Regulators during Early Ocular Development and in the Post-Mitotic Retina

Linda Vuong, Daniel E. Brobst, Anisse Saadi, Ivana Ivanovic, and Muayyad R. Al-Ubaidi

PURPOSE. Because of its role in cell cycle regulation and apoptosis, p53 may be involved in maintaining the post-mitotic state of the adult eye. To shed light on the role of p53 in retinal development and maintenance, this study investigated the pattern of expression of p53, its family members, and its regulators during the development of the mouse eye.

METHODS. Relative quantitative real-time PCR (qRT-PCR) was used to determine the steady-state levels of target transcripts in RNA extracted from wild-type mouse whole eyes or retinas between embryonic day (E) 15 and post-natal day (P) 30. Immunoblotting was used to compare the steady-state levels of the protein to that of the transcript.

RESULTS. Transcript and protein levels for p53 in the eye were highest at E17 and E18, respectively. However, both p53 transcript and protein levels dropped precipitously thereafter, and no protein was detected on immunoblots after P3. Expression patterns of p63, p73, Mdm2, Mdm4, and Yy1 did not follow that of p53. Immunohistochemistry analysis of the developing eye showed that both p53 and Mdm2 are abundantly expressed at E18 in all layers of the retinal neuroblast.

CONCLUSIONS. Downregulation of p53 in the post-mitotic retina suggests that, although p53 may be involved in ocular and retinal development, it may play a minimal role in healthy adult retinal function. (*Invest Ophthalmol Vis Sci.* 2012; 53:4821–4831) DOI:10.1167/iovs.11-8681

The p53 tumor suppressor plays a critical role in regulating DNA damage repair, cell cycle progression, apoptosis, and autophagy.¹ It is also involved in the regulation of significant physiological steps during development, aging, and metabolism (for review, see ref. 1). During retinal genesis, developmental apoptosis is observed from embryonic day (E) 15 until post-natal day (P) 11.² This indicates that at least during development, there may be a role for p53 in the retina.

From the Department of Cell Biology, University of Oklahoma Health Sciences Center, Oklahoma City, Oklahoma

Supported by the Foundation Fighting Blindness (MRA), National Center For Research Resources Grant P20RR017703, and National Eye Institute Grants P30EY12190 and R01EY018137 (MRA). The contents are solely the responsibility of the authors and do not necessarily represent the official views of National Institutes of Health or any of its institutes.

Submitted for publication September 28, 2011; revised April 13 and May 17, 2012; accepted June 13, 2012.

Disclosure: L. Vuong, None; D.E. Brobst, None; A. Saadi, None; I. Ivanovic, None; M.R. Al-Ubaidi, None

Corresponding author: Muayyad R. Al-Ubaidi, Department of Cell Biology, University of Oklahoma Health Sciences Center, BMSB 781, 940 Stanton L. Young Boulevard, Oklahoma City, OK 73104; muayyad-al-ubaidi@ouhsc.edu.

p53 is negatively regulated by murine double minute 2 (Mdm2),¹ Mdm4,³ and yin yang 1 (Yy1).⁴ Downstream targets of p53 include p21, a Cip/Kip cyclin-dependent kinase (Cdk) inhibitor⁵ essential for p53-dependent cycle arrest,⁶ the retinoblastoma protein (pRb),⁷ and the E2F family of transcription regulators.⁸

Although p53 has been shown to be expressed in several murine ocular tissues,^{9,10} p53 knockout mice on C57BL × CBA¹¹ and 129/Sv × C57BL/6¹² backgrounds do not exhibit any ocular abnormalities, implying that p53 may not be essential for ocular development.¹¹ However, severe abnormalities are present in p53 null mice on the pure BALB/c OlaHsd¹³ and C57BL/6¹⁴ backgrounds, suggesting that alleles from the C57BL/6 genetic background interact with p53 in ocular development and contribute to the abnormal phenotype observed in the absence of p53.¹⁴

In terms of ocular stress and disease, p53 has been shown to be involved in the retinal response to oxidative stress^{15,16} and to lead to G₁ arrest upon retinal exposure to ionizing radiation.^{17–19} p53 may also play a role in hypoxia due to ischemia^{20,21} and the development of age-related macular degeneration.²² In contrast, p53 is not directly involved in the apoptotic response to intense light damage^{23,24} or retinitis pigmentosa.^{25–27} Finally, although p53 mutations are not associated with retinoblastoma, p53 does play a role in the disease development. In retinoblastoma cells, the p53 negative regulator Mdm4 is overexpressed, leading to p53 degradation and allowing cancerous cells to bypass the p53 checkpoint.²⁸ For a review of the known roles of p53 in ocular stress, please see ref. 29.

To begin to understand the role of p53 and its family members, regulators, and downstream target genes in the eye, the current study examined the levels of the aforementioned genes during early mouse eye development and in the post-mitotic retina. Using quantitative real-time PCR (qRT-PCR), immunoblotting, and immunohistochemistry (IHC) analysis, we determined the steady-state levels of the transcript and protein of p53 and of its regulators Mdm2, Mdm4, and Yy1, either in whole eyes from E15 through P3 or in retinal samples after P3 through P30 from C57BL/6 mice, which have been shown to develop ocular abnormalities in the absence of p53.¹⁴ To determine whether other family members play any potential role in absence of p53, levels of p63 and p73 were also examined. Finally, expression levels of downstream p53 target genes were investigated.

MATERIALS AND METHODS

Animals

C57BL/6 mice were housed and fed as previously described.³⁰ To obtain eyes from embryonic stages, female mice were superovulated and mated to proven male breeders.³⁰ Eyes were obtained from fetuses

TABLE 1. Primers Used for qRT-PCR

Gene	Accession Number	Direction	Primer Sequence (5' → 3')	Efficiency (%)	Amplicon (bp)
<i>Trp53</i>	NM_011640	F	TGCTCACCCCTGGCTAAAGTT	98	269
		R	GTCCATGCAGTGAGGTGATG		
<i>Mdm2</i>	NM_010786	F	TGCAAGCACCTCACAGATTC	87	235
		R	GAAACTCGGGACTCCAAACA		
<i>Yy1</i>	NM_009537	F	TGAGAAAGCATCTGCACACC	107	212
		R	ATAGGGCCTGTCTCCGGTAT		
<i>Mdm4</i>	NM_008575	F	CTGCCTTGGTGGTTTTCTAGG	121	254
		R	TCATCATCCTTTCCACCTC		
<i>Trp63</i>	NM_011641	F	GTCAGCCACCTGCACGTATT	77	202
<i>Trp73</i>	NM_011642	F	CTCATTGAACTCACGGCTCA	120	250
		R	CAAGGTACACGGTGGTGTCA		
<i>Cdkn1a</i>	NM_007669	F	CCTTGGGAAGTGAAGCACTC	109	206
		R	GTACTTCCTCTGCCCTGCTG		
<i>Pcna</i>	NM_011045	F	GGGCACTTCAGGGTTTTCTC	93	208
		R	CCACATTGGAGATGCTGTTG		
<i>Tert</i>	NM_009354	F	CAGTGGAGTGGCTTTTGTGA	111	295
		R	AGGGTAAGCTGGTGGAGGTT		
<i>Rb</i>	NM_009029	F	ACACTGTGACGCAGGAAGTG	119	263
		R	TGCATGGCTTTTTCAGATTCAC		
<i>p107</i>	NM_011249	F	ACAGGGCAAGGGAGGTAGAT	89	282
		R	TCATTTGTGTTGGGCACAGT		
<i>p130</i>	NM_011250	F	TACACCCAGGGGAACTCAG	89	243
		R	GAAAGCGTGCAATGTCTGAA		
<i>E2f1</i>	NM_007891	F	TGCCACTACCACAAATGGAA	116	211
		R	ACTGTGACTTTGGGGACCTG		
<i>E2f3</i>	XM_127250	F	CCCATTTTGGTCTGCTCAAT	114	242
		R	GCTGTACCCTGGACCTCAA		
<i>E2f4</i>	NM_148952	F	GGTCTGTGTGTTTCCGTCT	99	285
		R	AGCTCAAGGCAGAGATCGAG		
<i>E2f5</i>	NM_007892	F	TAGGCCCACTCATGCTCTTT	95	238
		R	GTGGCTACAGCAAAGCATCA		
<i>Hprt</i>	NM_013556	F	CACATGGATAGGCCCTGAGT	100	152
		R	GCAAACCTTGTCTTCCCTGGTT		
		R	CAAGGGCATATCCAACAACA		

Amplification efficiency was determined by the calibration dilution curve and slope calculation. This calculation uses the slope produced by a quantitative PCR standard curve to determine the efficiency of the PCR reaction. Efficiency (E) is calculated from the equation $E = -1 + 10^{(-1/\text{slope})}$. Slopes between -3.1 and -3.6 giving reaction efficiencies between $\sim 80\%$ and $\sim 120\%$ are typically acceptable. F, forward; R, reverse.

at the specified time points post-coitus. All experiments involving animals were approved by the local Institutional Animal Care and Use Committees and conformed to the National Institute of Health Guide for the Care and Use of Laboratory Animals and the Association for Research in Vision and Ophthalmology Resolution on the Use of Animals in Research.

Relative qRT-PCR

Quantitative real-time PCR was performed as previously described³¹ with total RNA extracted from C57BL/6 tissue. For E15 through P3, whole eyes were used. For time points after P3, retinas were extracted. Primers for all genes were designed to span introns to avoid amplification from genomic DNA.

Two qRT-PCR assays were performed in triplicate with 0.2 μg of each cDNA sample, using the gene-specific primer pairs shown in Table 1. ΔCt values were calculated relative to those of the neuronal housekeeping gene encoding hypoxanthine phosphoribosyltransferase (*Hprt*). *Hprt* was assigned an arbitrary expression level of 10,000. Relative gene expression values were calculated as follows: relative expression = $10,000/2^{\Delta\text{Ct}}$, where $\Delta\text{Ct} = (\text{gene Ct} - \text{Hprt Ct})$. PCR quality and specificity were verified by melting curve dissociation analysis and gel electrophoresis.

Amplification efficiency was determined by the calibration dilution curve and slope calculation. This calculator uses the slope produced by a qPCR standard curve to calculate the efficiency of the PCR. Multiple

5-fold dilutions of the cDNA are made, and PCRs are performed with a primer set. cT values are determined and plotted against log starting cDNA concentration by using a scatter chart (Excel software; Microsoft, Redmond, WA) and the slope was determined. Efficiency (E) is calculated from the equation: $E = -1 + 10^{(-1/\text{slope})}$. Slopes between -3.1 and -3.6 giving reaction efficiencies between $\sim 80\%$ and $\sim 120\%$ are typically acceptable. Except for p63 (Table 1), all primer sets produced PCR efficiencies within the acceptable range.

Immunoblot Analysis

Whole eyes or retinas were isolated (depending on age, as described above) and processed for immunoblotting as previously described.³⁰ Blots were incubated with a primary antibody at specified dilutions (Table 2), washed, and then incubated with a secondary antibody. Membranes were incubated with SuperSignal enhanced chemiluminescent detection system (Pierce, Rockford, IL) and imaged using a Kodak image station (Carestream Molecular Imaging, Rochester, NY).

Cell Lines

Cone photoreceptor-derived 661W cells³² were grown in Dulbecco's modified Eagle's medium (Invitrogen, Carlsbad, CA) supplemented with 10% fetal bovine serum (Cellgro, Herndon, VA) and a 1% antimycotic-antibiotic cocktail (Invitrogen) and maintained in a humidified atmosphere of 95% air and 5% CO_2 at 37°C.

TABLE 2. Antibodies Used for Protein Detection

Antigen	Dilution	Source	Catalog Number	Molecular Mass (kDa)
p53	1:100	Santa Cruz Biotechnology	sc-6243	53
Mdm2	1:500	EMD Biosciences	OP46	57
Yy1	1:100	Santa Cruz Biotechnology	sc-1703	45
Mdm4	1:500	Dr. Steven J. Berberich, Boonshoft School of Medicine, Wright State University, Dayton, OH		70
p63	1:500	Abcam	ab53039	63
p73	1:100	Santa Cruz Biotechnology	sc-7957	73
p21	1:100	Santa Cruz Biotechnology	sc-397	21
PCNA	1:100	Oncogene Science	NA04	34
Tert	1:100	Santa Cruz Biotechnology	sc-7212	134
pRb	1:1000	Santa Cruz Biotechnology	sc-50	110
p107	1:200	Abcam	ab2451	121
p130	1:100	Santa Cruz Biotechnology	sc-317	130
E2F1	1:1000	Santa Cruz Biotechnology	sc-251	55
E2F3	1:400	Abcam	ab74180	49
E2F4	1:500	Abcam	ab53060	44
E2F5	1:1000	Abcam	ab44996	58
Actin	1:2000	Abcam	ab6276	42

MCF-7 breast cancer cells³³ were grown in the same medium and under the same conditions as described above. NIH-3T3 cells, a mouse embryonic fibroblast cell line,³⁴ is the recommended positive control for p107 and were grown in the same medium and under the same conditions as described above.

Immunohistochemistry

IHC analysis was performed with frozen sections of eyes as described previously.³¹ Labeling with the antibodies listed in Table 3 was visualized using an Olympus BX-62 microscope equipped with a spinning disc confocal unit (Olympus America, Center Valley, PA) and an Orca-ER camera (Hamamatsu, Bridgewater, NJ). Images were acquired using Slidebook version 4.2 software (Intelligent Imaging Innovations, Denver, CO). Figures were assembled in Adobe Photoshop CS (Adobe, Mountain View, CA), and brightness, contrast, and threshold were adjusted to highlight specific labeling.

Statistical Analysis

Unless otherwise stated, statistical significance was determined by using one-way ANOVA with Bonferroni post hoc multiple pairwise comparison tests (Prism; GraphPad Software, San Diego, CA), and data are means \pm standard error of the means (SEM). Statistical significance was set at a *P* value of <0.05.

RESULTS

Expression of p53 and Its Regulators during Mouse Retinal Development

To better understand the developmental role of p53 and its family members, regulators, and target genes, their expression levels during murine retinal development were examined.

The transcript for *Trp53*, the murine p53 gene, was detected at E15 with a significant increase at E17, followed by a gradual decrease until P30, when *Trp53* expression reached its lowest level (Fig. 1A, upper panel). The reduction in *Trp53* expression after P11 may be biologically meaningful because retinal mitosis and normal developmental apoptotic cell death are both completed at this time.² This pattern of expression implies that *Trp53* may play a role in either the division and/or differentiation of retinal progenitor cells or in developmental apoptotic death.

At the protein level, P53 was abundant at E18 in quantities comparable to those observed in the continuously dividing cone photoreceptor-derived cell line 661W (Fig. 1A, lower panel). At P3, P53 is still detectable but at a significantly lower level than that at E18. At subsequent time points during which the retina alone was analyzed, P53 protein was barely visible. This suggests that either p53 is unnecessary for retinal development at later stages or that p53 is more abundantly expressed at earlier time points in other ocular structures.

Mdm2, Mdm4, and Yy1 are well-known negative regulators of p53.³⁵ *Mdm2* transcript levels significantly increased from E15 to P1 and remained steady between P3, when the whole eye was analyzed, and at P7, when analysis of the retina alone began. After P7, levels of *Mdm2* transcript fell, and thereafter, transcript levels remained stable into adulthood. However, in contrast to P53 which peaked at E18, *Mdm2* protein levels seem to peak between P3 and P7 and then decline slightly (Fig. 1B, lower panel). The increase in protein expression at P3 and P7 reflects the peak in transcript levels (Fig. 1B).

Comparably to *Trp53*, transcript levels for *Yy1* increased after E15 in ocular tissues and dropped shortly after birth. In the P7 retina, levels of *Yy1* transcript were insignificantly lower than ocular levels at P3 but continued to drop as the retina progressed in development (Fig. 1C, upper panel). Yy1

TABLE 3. Antibodies Used for Immunohistochemistry

Antigen	Dilution	Source	Catalog Number
Polyclonal p53	1:50–1:500	Santa Cruz Biotechnology	sc-6243
Monoclonal p53	1:10	Oncogene Research Products	OP29
Monoclonal p53	1:2000	Cell Signaling Technology	2524
Monoclonal Mdm2	1:20–1:100	Oncogene Research Products	OP46

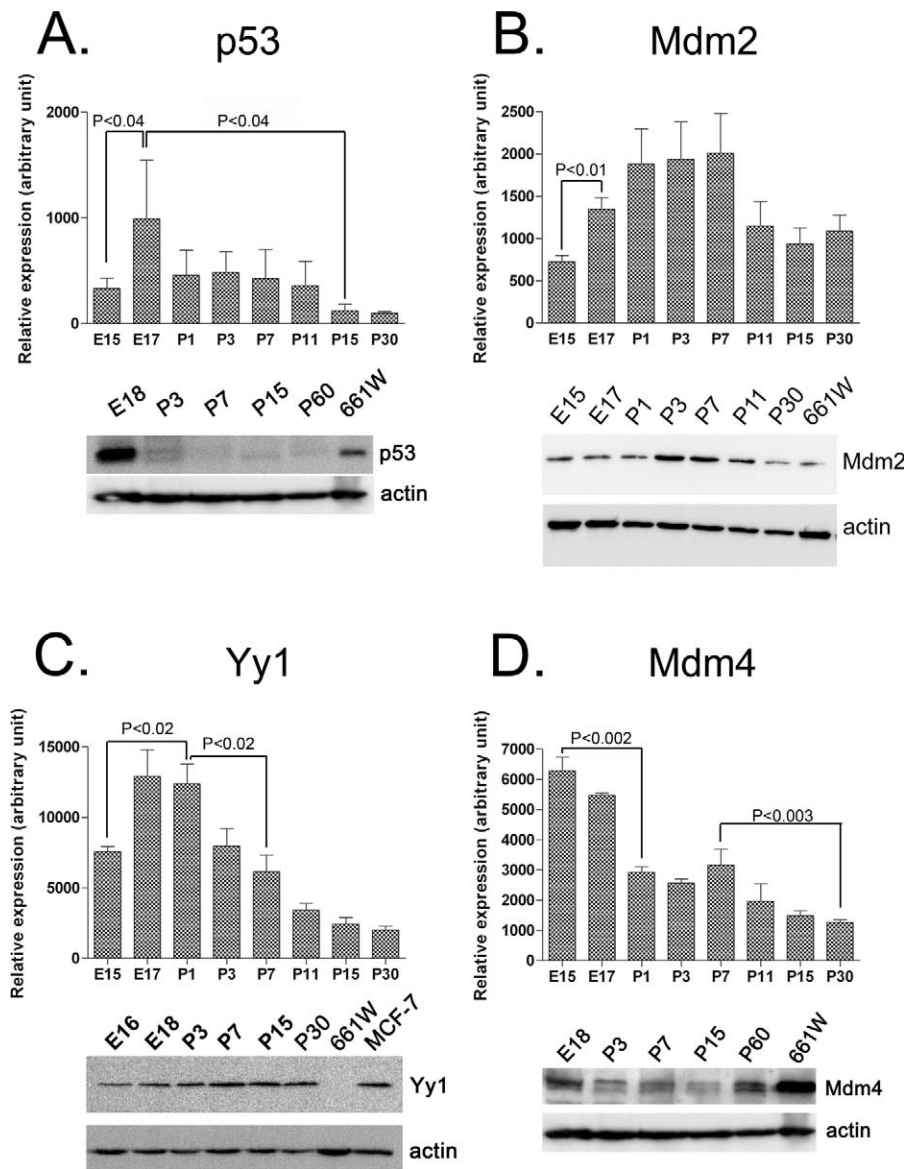


FIGURE 1. Pattern of expression of *Trp53*, its protein product, and its regulators in the developing mouse eye and retina. qRT-PCR for *Trp53* (A, upper panel), *Mdm2* (B, upper panel), *Yy1* (C, upper panel), and *Mdm4* (D, upper panel) was performed, and each presented value was determined from two independent analyses, each performed in triplicate with four independent samples. Data were plotted using Prism software. Error bars represent standard deviations. Whole eyes (E15–P3) or retinas (P7 and later) were obtained from mice at time points throughout development. Immunoblotting analysis ($n = 4$ for A; 3 for B; 3 for C; and 2 for D) of protein products of genes of interest was performed using the corresponding antibodies (lower panels). 661W, a cone photoreceptor cell line, and MCF-7, a breast cancer cell line, were used as positive controls. Fifty micrograms of sample protein extracts and 30 μ g of control cell lysates were loaded in each corresponding lane.

protein, on the other hand, was expressed starting at embryonic stages and increased until P7 to the level at which the protein was maintained at the later time points examined (Fig. 1C, lower panel). Because the retina became totally post-mitotic by P11,³⁶ it seems that Yy1 levels increased as the cells differentiated and entered post-mitosis. This is supported by the fact that the continuously dividing 661W cell line does not express any Yy1. This also suggests that Yy1 may have an alternative function in the retina other than p53 regulation.

Mdm4 transcript levels in ocular tissues were high at E15 and gradually decreased thereafter (Fig. 1D, upper panel). However, at P7, retinal levels of *Mdm4* transcript were slightly higher than those observed in total ocular tissues at P3. At later post-natal stages, retinal *Mdm4* levels declined slowly, and by P30, they were significantly lower than the levels observed at

P7. The level of Mdm4 protein reflects the pattern observed for its transcript (Fig. 1D, lower panel). However, there was an increase at P60 that is hard to explain if the only function for Mdm4 is regulation of p53, because P53 is almost undetectable in adult retinal extracts. Nevertheless, in embryonic and early post-natal stages, Mdm4 behaved in a pattern similar to that of P53, suggesting that Mdm4 rather than Mdm2 may be the actual regulator of retinal p53.

To determine whether *Trp53* was expressed mostly in the retina or in other ocular tissues during embryonic developmental time points, IHC analysis was performed. As shown in Figure 2, both P53 and Mdm2 were abundantly present at E18 in the neuroblast layer, which is in agreement with prior immunoblot results (Figs. 1A, 1B). However, while Mdm2 is clearly present in the retinal pigment epithelium, P53 is absent

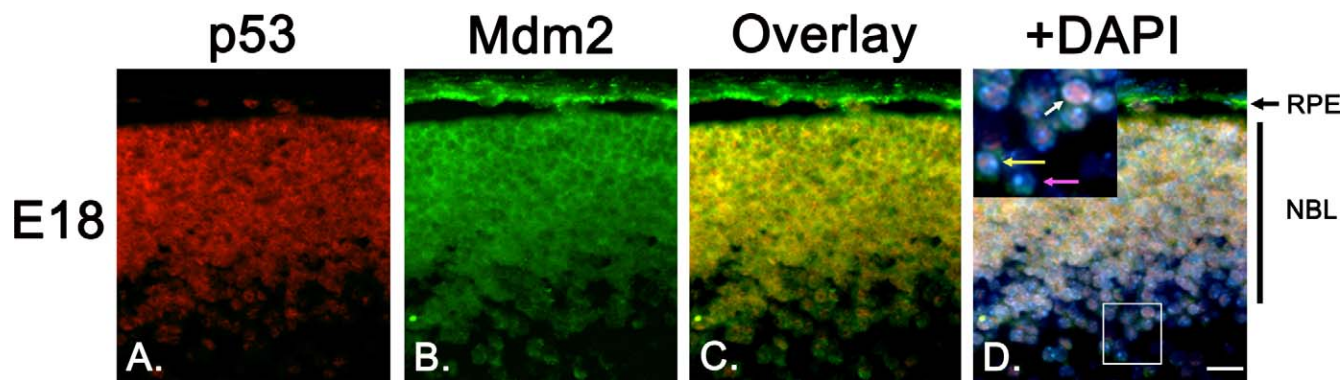


FIGURE 2. IHC localization of P53 and Mdm2. Frozen sections of wild-type retinas were probed using antibodies against P53 (red) and Mdm2 (green) at E18. Nuclei are counterstained with 4',6-diamidino-2-phenylindole (blue). Labeling of P53 and Mdm2 is abundant in the retina at E18 (A and B), and many cells show coexpression in the neuroblastic layer (C). However, the RPE seems to express only Mdm2 (B). The area marked with a white box is enlarged in the inset (D). Some retinoblasts may only express P53 (D, inset, white arrow). P53 is found mostly in the nucleus (D, white and yellow arrows in inset), while Mdm2 is localized mostly to the cytoplasm (D, pink and yellow arrows in inset). Bar = 50 micrometers.

(Fig. 2, compare panels A and B). In the retinoblast layer, most cells coexpressed these two proteins. However, there were cells (Fig. 2D, white arrow) that expressed P53 alone while other cells expressed Mdm2 alone (Fig. 2D, pink arrow). Furthermore, P53 generally appears to be localized to the nucleus (Fig. 2D, white and yellow arrows), and Mdm2 seems to be mostly cytoplasmic (Fig. 2D, yellow and pink arrows).

Expression of p53 Family Members during Retinal Development

The p53 family also includes p63³⁷ and p73.^{38,39} As structural and functional homologs of p53, these family members can form oligomers, bind DNA, and activate p53 target genes to regulate the cell cycle and mediate apoptosis.^{37–40} p63 is required for ectoderm-derived tissues to develop normally,^{41,42} and loss of p73 leads to hydrocephalus, chronic inflammation, and defects in neuronal development and pheromone sensing in zebrafish embryos,⁴³ suggesting a potential functional redundancy in the roles of p53, p63, and p73 in retinal development. Therefore, the patterns of expression of *Trp63* and *Trp73* transcripts during retinal development were determined.

qRT-PCR showed that *Trp63* was expressed at relatively high levels in ocular tissues at E15 but rapidly and significantly dropped at E17. *Trp63* expression dropped further at P1 but remained steady at P3. A second dramatic drop in expression was observed at P7 in retinal samples, to levels that were almost undetectable, which continued into early adulthood (Fig. 3A, upper panel). Immunoblot analysis showed that in contrast to transcript levels, P63 protein levels were mostly stable throughout all developmental stages tested. (Fig. 3A, lower panel). However, there might have been a slight increase in P63 levels at P7. Of interest is the fact that P63 was barely observed in 661W cells, which express reasonable amounts of P53 (Fig. 1A, lower panel). The pattern of expression of *Trp63* transcript suggests that P63 might play a minimal role in early ocular and/or retinal development, at least in the presence of P53.

Expression of *Trp73* transcript is remarkably different than those of *Trp53* and *Trp63*. Although it also started at relatively high levels at E15, *Trp73* transcript levels dropped significantly by E17 and remained at that level through P1. However, at P3, there was a significant increase in transcript steady-state levels before dropping again to a drastically low level by P7. Although *Trp73* transcript levels were virtually undetectable at P7, they rebounded slightly at P15 and P30 (Fig. 3B, upper panel). At

the protein level, P73 started at relatively high levels at E16 but quickly became undetectable after E18 in ocular tissues and the retina (Fig. 3B, lower panel). This suggests that p73 may not play any significant role in mouse ocular/retinal late development, at least in presence of p53. However, based on the high levels of p73 that were observed at E16, P73 may have a significant role in early ocular development.

Expression of p53 Target Genes during Retinal Development

Because p53 has been shown to be tightly regulated during retinal development, it was relevant to examine the pattern of expression of p53 targets including p21, pRb, and the E2F family. p53 regulates cell cycle arrest at G₁ through p21-mediated inactivation of pRb.⁴⁴ p21-mediated cell cycle arrest can also occur through downregulation of p21 by telomerase reverse transcriptase (TERT) in response to dysfunctional telomeres⁴⁵ and through inhibition of proliferating cell nuclear antigen (PCNA), an essential DNA polymerase δ cofactor.^{46,47}

qRT-PCR analysis showed that transcript levels of *Cdkn1a*, the murine p21 gene, were relatively high between E15 and P3, when the whole eye was examined, and were then subsequently reduced to lower levels that were maintained from P7 and beyond, when the retina alone was examined (Fig. 4A, upper panel). Current data suggest a role for p21 in the development of ocular tissues other than the retina. However, P21 was not observed in any of the protein samples obtained from ocular or retinal tissues (Fig. 4A, lower panel). Clearly, P21 does not follow the pattern observed for its transcript. It is interesting that P21 is also absent in 661W cells. Altogether, the data suggest that *Cdkn1a* may serve a role in *Trp53*-dependent stress response such as apoptosis.

The developmental pattern of expression of *Pcna* transcript resembled that of *Trp53*, with high expression at E17 that was reduced to very low levels by P11 (Fig. 4B, upper panel). However, the protein levels seemed to be steady when ocular tissues were examined between E16 and P3 but lower in retinal samples at P7 and almost nonobservable at P30. At P7, central portions of the retina have entered post-mitosis,³⁶ and by P30 all retinal cells stopped dividing.³⁶ This pattern is in agreement with previous IHC findings⁴⁸ and correlates well with retinal cell cycle activity.

Examination of the *Tert* expression pattern shows that steady-state transcript levels fluctuated in ocular tissues between E15 and P3 (Fig. 4C, upper panel). However, levels of *Tert* transcript seemed to drop as retinal cells exited the cell

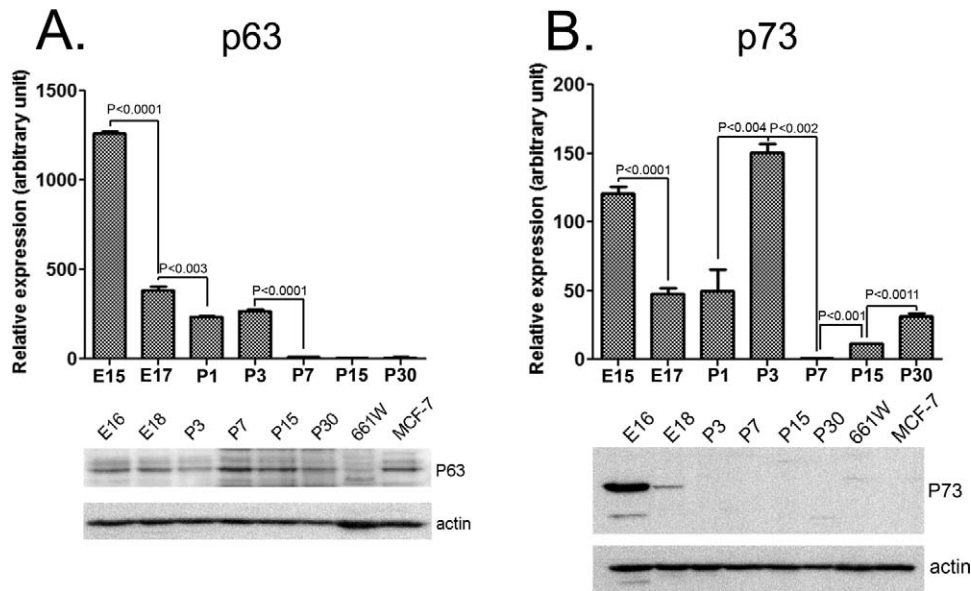


FIGURE 3. Pattern of expression of p53 family members in the developing mouse eye and retina. qRT-PCR for *Trp63* (A, upper panel) and *Trp73* (B, upper panel) was performed, and each presented value was determined from two independent analyses each performed in triplicate on four independent samples. Data were plotted using Prism software. Error bars represent standard deviations. Whole eyes (E15–P3) or retinas (P7 and after) were obtained from mice at time points throughout retinal development. Immunoblotting analysis ($n = 3$ for A; 3 for B) of protein products for the genes of interest was performed using the corresponding antibodies (lower panels). 661W, a cone photoreceptor cell line, and MCF-7, a breast cancer cell line, were used as positive controls. 50 μg of sample protein extracts and 30 μg of control cell lysates were loaded in each corresponding lane.

cycle by P11 (Fig. 4, upper panel). On the protein level, Tert levels increased from E16 to P3, but, unlike the transcript levels that seemed moderately high in the retina at P7, the protein levels were reduced at P7. Surprisingly, Tert levels were increased at P15 and then drop to very low levels by P30 (Fig. 4, lower panel). It is difficult to propose a function for Tert at

P15 as the entire retina is post-mitotic by that age.³⁶ Although there was one band observed in MCF-7 cells, ocular tissues seemed to express multiple forms of Tert, with a prominent larger form.

What is interesting is that despite being downstream targets of p53, expression patterns of *Cdkn1a* and *Tert* message did

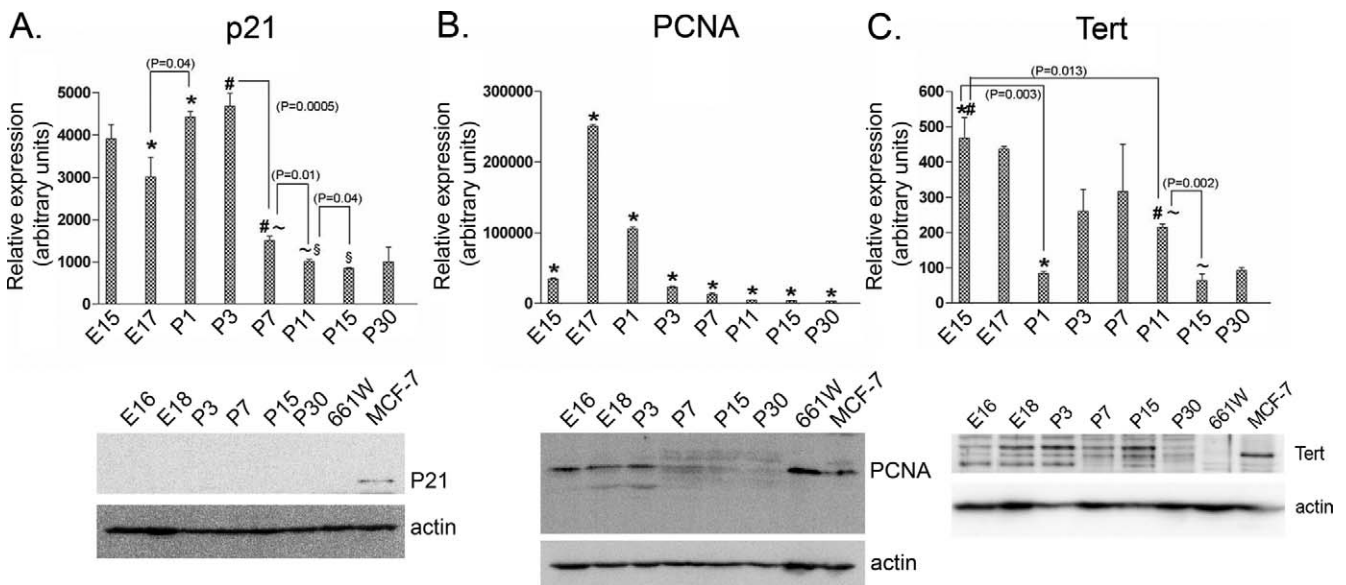


FIGURE 4. Pattern of expression of p21, PCNA, and Tert in the developing mouse eye and retina. qRT-PCR for *Cdkn1a* (A, upper panel), *Pcna* (B, upper panel), and *Tert* (C, upper panel) was performed, and each presented value was determined from two independent analyses each performed in triplicate on four independent samples. Data were plotted using Prism software. Error bars represent standard deviations. Whole eyes (E15–P3) or retinas (P7 and after) were obtained from mice at time points throughout retinal development. Immunoblotting analysis ($n = 3$ for A; 3 for B; 3 for C) of protein products for the genes of interest was performed using the corresponding antibodies. 661W, a cone photoreceptor cell line, and MCF-7, a breast cancer cell line, were used as positive controls. 50 μg of sample protein extracts and 30 μg of control cell lysates were loaded in each corresponding lane.

not follow that of *Trp53* transcript. Furthermore, although the decline in the transcript levels of p53 target genes was consistent with their role in cell cycle regulation, it is difficult to understand the behavior of their equivalent proteins. Altogether, this suggests that regulation of these genes may be controlled by additional transcription factors.

Recent evidence shows a strong correlation between the functionality of the p53 pathway and the development of retinoblastoma,²⁸ leading us to examine the developmental patterns of expression of pRb, its family members p107 and p130, and its targets E2F1, E2F3, E2F4, and E2F5. Support for a developmental role of the retinoblastoma pathway is further highlighted by the early age of onset of retinoblastoma in cases where *Rb* is mutated.

Expression of the *Rb* transcript started at relatively low levels at E15 but increased by E17 before gradually decreasing to a steady level after P11, when the development of the retina was complete (Fig. 5A, upper panel).³⁶ On the protein level, pRb levels increased moderately at E18 but then remained detectable as late as P30 (Fig. 5B, lower panel), suggesting a role for pRb beyond control of the cell cycle in the post-mitotic retina.

p107 transcript levels were high from E15 through P1, with a statistically insignificant reduction at P3 (Fig. 5B, upper panel). The *p107* levels dropped significantly by P11 and remained low at all later time points. The pattern of protein expression closely followed the pattern observed for the transcript (Fig. 5B, lower panel). It is clear that P107 levels are modulated with the cell cycle activity more so than pRb, suggesting that P107 may play a significant role during ocular/retinal development in the mouse. This is in agreement with the role described for p107 as a functional alternative to pRb in the *Rb* protein-deficient mouse.⁴⁹

Although *p130* transcript levels fluctuated during ocular/retinal development, they were maintained at relatively high levels. That the levels of *p130* transcript were relatively high at P30, when expression of both *Rb* and *p107* were at their lowest during retinal development, may suggest a role for p130 in the post-mitotic retina. This is consistent with previous work showing that p130 is high in arrested cells.⁵⁰ This is also consistent with the relatively low, constant levels of P130 observed throughout all stages of ocular/retinal development tested (Fig. 5C, lower panel).

The retinoblastoma family of proteins regulates the activity of the E2F protein family to arrest the cell cycle at G₁.⁵¹ pRb binds all E2F proteins, while p107 and p130 bind specifically to the E2F3b, -4, -5, -6, -7a, and -7b transcriptional repressors.⁵² We detected higher levels of *E2f1* transcript and protein between E15 and P3 (Fig. 6A). The subsequent decrease in transcript expression at P7 onward was reflected in the protein level (Fig. 6A). Although pRb levels remained constant during these time points (Fig. 5A, lower panel), levels of P107 were considerably high (Fig. 5B, lower panel). pRb is known to bind to and inactivate E2F1,^{53,54} implying that the increase in E2F1 may have been the result of gene expression driven by a cell cycle protein not included in this study.

E2f3 transcript levels remained generally steady, with peaks of expression at E17 and P11 (Fig. 6B, upper panel). The increase in *E2f3* expression at E17 coincided with the E17 increase observed in the *Trp53* transcript (Fig. 1A, upper panel). The largest amount of protein was observed in the retina at P7 (Fig. 6B, lower panel).

In contrast, *E2f4* transcript was maintained at constant levels throughout development with a statistically significant reduction apparent only at P30 (Fig. 6C, upper panel). The protein seemed to be expressed at constant low levels (Fig. 6C, lower panel).

Finally, although levels of *E2f5* transcript varied with the progression of ocular/retinal development (Fig. 6D, upper panel), the protein levels seemed to remain constant throughout the time points examined (Fig. 6D, lower panel).

DISCUSSION

To examine the role of p53 in ocular/retinal development and maintenance, transcript and protein steady-state levels for p53, its family members, regulators, and downstream targets were analyzed by qRT-PCR and immunoblotting. This study is especially relevant because the retina becomes post-mitotic by P11,² suggesting a role for p53 in cell cycle arrest. Furthermore, because programmed cell death is observed during the development of ocular tissues, p53 may also play a role in apoptosis of the developing eye. This study was performed in the C57BL/6 mouse because it is the strain that has been shown to develop ocular abnormalities in the absence of p53.¹⁴

Error-free execution of the fundamental process of cell division is essential for the continuity of all living organisms. An increase in ocular P53 at late embryonic stages implies that p53 may play a regulatory role in keeping developing ocular cells in check. As cells reach a post-mitotic state, P53 levels decrease to barely detectable levels. However, the expression pattern of the p53 negative regulators Mdm2, Mdm4, and Yy1 did not follow that of P53. The relatively higher expression levels of these regulatory proteins suggest either that high levels are necessary to effectively negatively regulate p53 or that these proteins play other roles in addition to their regulation of p53.

An interesting observation made in our IHC analysis is that the retinal pigment epithelium (RPE) did not express P53 but abundantly expressed Mdm2. This further supports the notion that Mdm2 may play a role in RPE cellular homeostasis, independent of its role in p53 regulation.

Because knocking out p53 showed no ocular phenotype in the C57BL × CBA and 129/Sv × C57/BL6 backgrounds, investigators concluded that p53 plays no role in retinal development or maintenance.^{11,12} However, when p53 was later knocked down in BALB/c OlaHsd and C57BL/6 mice, researchers found severe ocular abnormalities such as hyaloid vasculature that does not regress by P35 or P42, as in wild-type mice, which is similar to persistent hyperplastic primary vitreous in humans, a high frequency of cataracts, fibrous retrolental tissue, vitreal opacities, retinal folding, and hypoplastic optic nerves.¹⁴ This finding led the authors to suggest that alleles from the C57BL/6 background may contribute to the ocular abnormalities seen in the absence of p53.¹⁴ Alternatively, the p53 family members p63 and p73 may compensate, leading to no observed phenotypic abnormalities. Both p63 and p73 have been found to induce cell cycle arrest and apoptosis in a manner similar to that of p53.⁵⁵ However, an increase in P73 levels preceded that of P53, and its levels dropped significantly when P53 was high, suggesting that P73 may play a role only in early ocular development. Because P63 is generally expressed at steady low levels throughout all developmental stages examined, it may not play a direct role in ocular/retinal development. However, that does not preclude the potential role for p63 in the absence of p53. In fact, the potential role of p73 in early retinal development and the presence of p63 may provide an explanation as to why retinal development continues unabated in the retinas of some p53 knockouts.

Like p53, pRb, p107, and p130 act as tumor suppressors, in part by inhibiting cell cycle progression.⁵⁶ Recent findings have shown that misregulation of the p53 pathway plays a major role in the formation of retinoblastoma tumors.²⁸ One

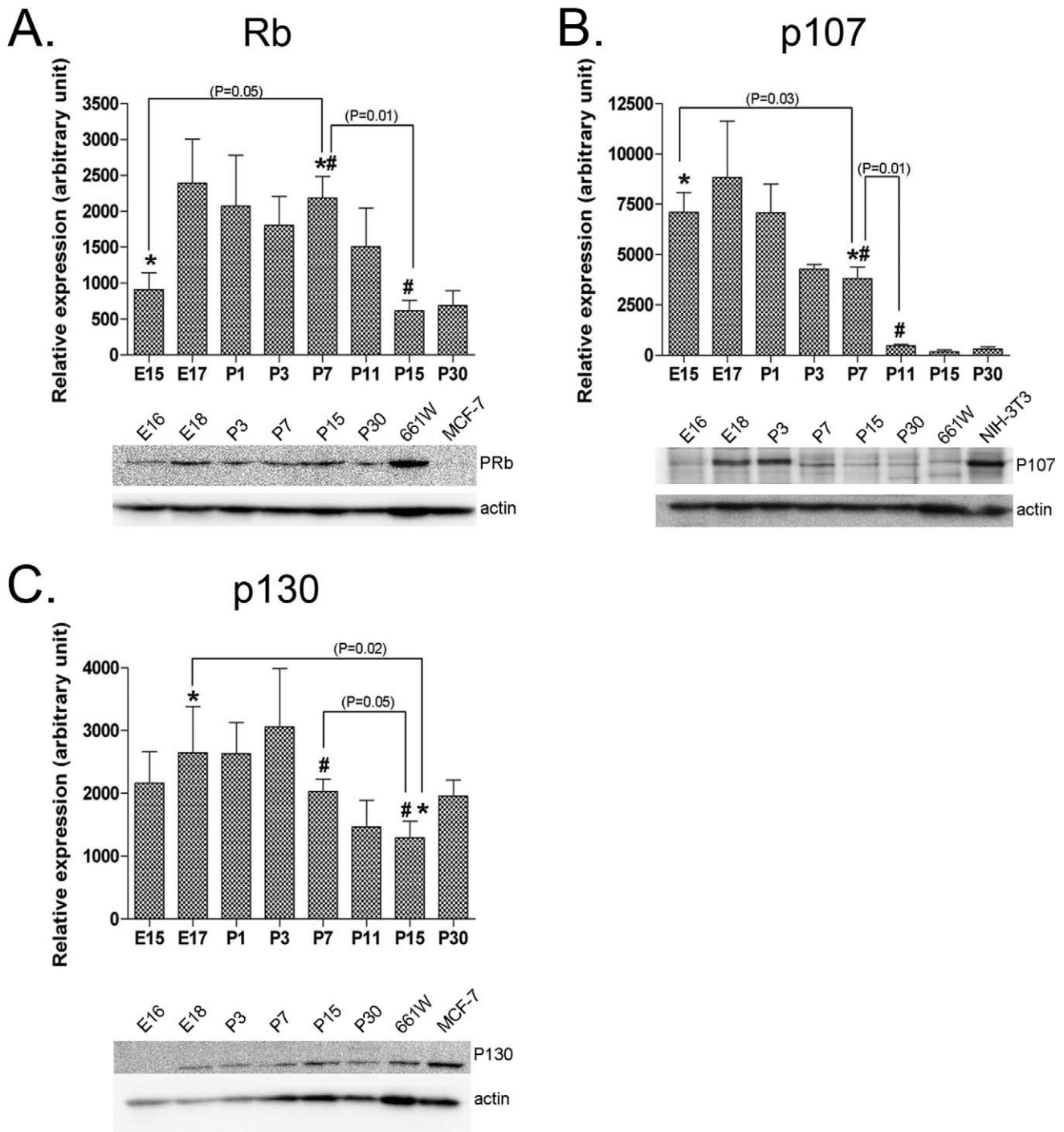


FIGURE 5. Pattern of expression of Rb, p107, and p130 in the developing mouse eye and retina. qRT-PCR for Rb (A, upper panel), p107 (B, upper panel), and p130 (C, upper panel) was performed, and each presented value was determined from two independent analyses each performed in triplicate on four independent samples. Data were plotted using Prism software. Error bars represent standard deviations. Whole eyes (E15–P3) or retinas (P7 and after) were obtained from mice at time points throughout retinal development. Immunoblotting analysis ($n = 3$ for A; 3 for B; 3 for C) of protein products for the genes of interest was performed using the corresponding antibodies. 661W, a cone photoreceptor cell line, MCF-7, a breast cancer cell line, and NIH-3T3, a mouse embryonic fibroblast cell line, were used as positive controls. 50 μ g of sample protein extracts and 30 μ g of control cell lysates were loaded in each corresponding lane.

would therefore expect that p53 and pRb are coregulated. However, the levels of p53 were highest at E18 and dropped precipitously thereafter, while the levels of pRb remained constant throughout the developmental stages studied. This suggests that despite its role in retinoblastoma, p53 plays an insignificant role in the regulation of pRb levels.

One observation from the analysis of transcript and protein levels is that while P53 protein levels more or less reflected that of the message, protein levels for the family members and regulators generally reflected neither the levels nor the pattern of message expression. This suggests translational and/or post-translational regulation of these proteins. This may have

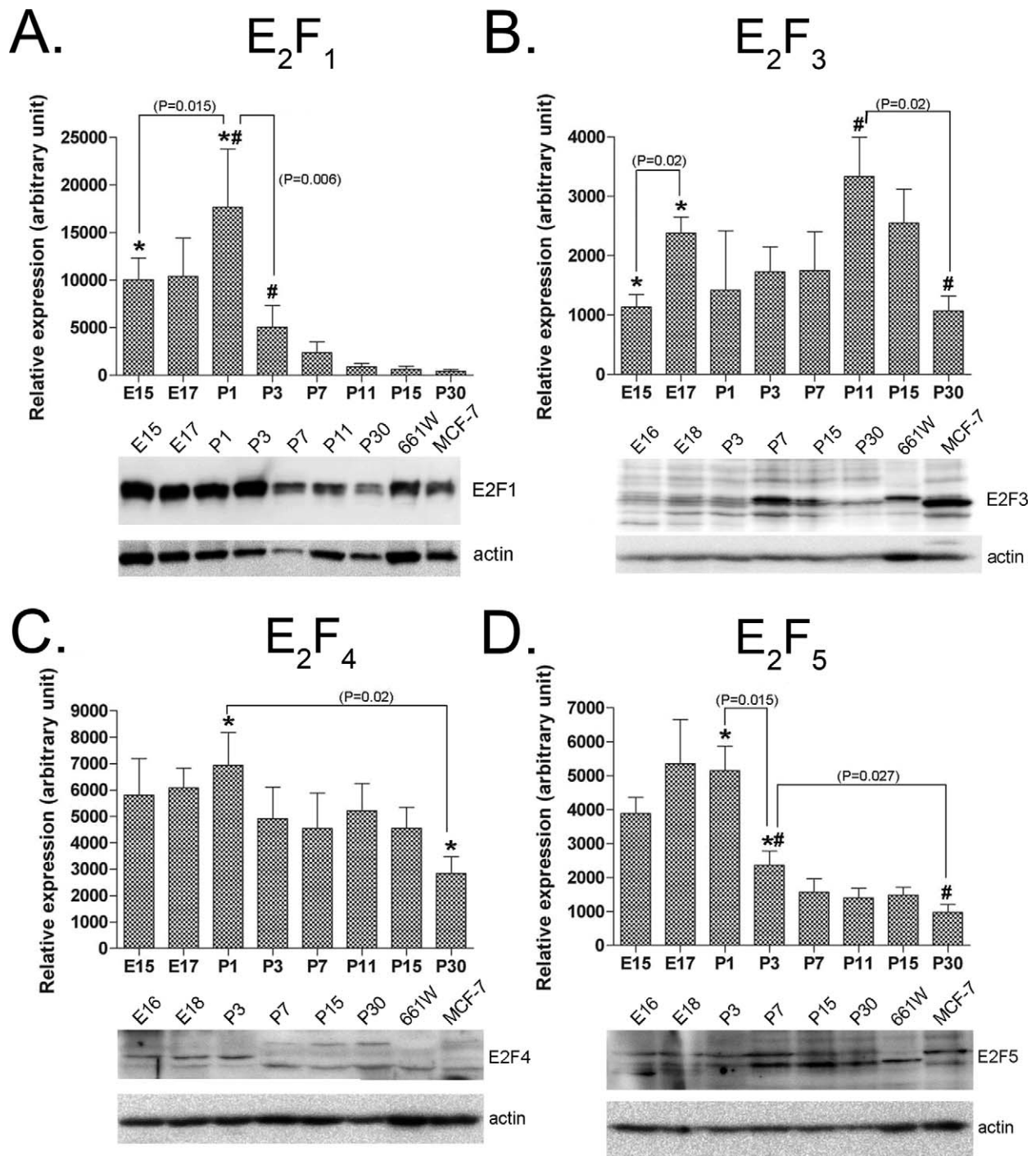


FIGURE 6. Pattern of expression of the E2F family in the developing mouse eye and retina. qRT-PCR for *E2f1* (A, upper panel), *E2f3* (B, upper panel), *E2f4* (C, upper panel), and *E2f5* (D, upper panel) was performed, and each presented value was determined from two independent analyses each performed in triplicate on four independent samples. Data were plotted using Prism software. Error bars represent standard deviations. Whole eyes (E15–P3) or retinas (P7 and after) were obtained from mice at time points throughout retinal development. Immunoblotting analysis ($n = 4$ for A; 3 for B; 3 for C, 3 for D) of protein products for the genes of interest was performed using the corresponding antibodies. 661W, a cone photoreceptor cell line, and MCF-7, a breast cancer cell line, were used as positive controls. Fifty micrograms of sample protein extracts and 30 μ g of control cell lysates were loaded in each corresponding lane.

biological implications whereby ocular/retinal cells can produce the necessary proteins when needed, such as upon stress. That speaks for the importance of p53 function(s) and the necessity for redundancies.

It has been shown that in response to DNA damage by ionizing radiation,^{18,19} p53 is phosphorylated, leading to

apoptosis.¹⁸ Therefore, it is possible that the only role for p53 in the adult retina is to induce apoptosis in response to damage. Such apoptotic cell death would reduce or prevent the immunological response that would be mounted should damaged retinal cells die via necrosis. However, not all retinal insults cause p53 activation. For example, the retinal response

to light damage is p53-independent,^{23,24} suggesting that the role of p53 in the retina may be quite specific.

In conclusion, expression of p53 and its family members, regulators, and downstream targets seems to occur mostly prior to ocular/retinal cells entering the post-mitotic state. This implies that, although some of these genes may play a role in retinal development, they play a minimal role, if any, in adult retinal function under normal unstressed conditions.

Acknowledgments

The authors thank Steven J. Berberich for the generous gift of Mdm4 antibody and Shannon M. Conley for critical evaluation of the manuscript.

References

- Aylon Y, Oren M. New plays in the p53 theater. *Curr Opin Genet Dev.* 2011;21:86-92.
- Cepko CL, Austin CP, Yang X, Alexiades M, Ezzeddine D. Cell fate determination in the vertebrate retina. *Proc Natl Acad Sci U S A.* 1996;93:589-595.
- Mancini F, Di CG, Monti O, et al. Puzzling over MDM4-p53 network. *Int J Biochem Cell Biol.* 2010;42:1080-1083.
- Gordon S, Akopyan G, Garban H, Bonavida B. Transcription factor YY1: structure, function, and therapeutic implications in cancer biology. *Oncogene.* 2006;25:1125-1142.
- Gartel AL, Tyner AL. The role of the cyclin-dependent kinase inhibitor p21 in apoptosis. *Mol Cancer Ther.* 2002;1:639-649.
- Niculescu AB III, Chen X, Smeets M, Hengst L, Prives C, Reed SI. Effects of p21(Cip1/Waf1) at both the G1/S and the G2/M cell cycle transitions: pRb is a critical determinant in blocking DNA replication and in preventing endoreduplication. *Mol Cell Biol.* 1998;18:629-643.
- Porrello A, Cerone MA, Coen S, et al. p53 regulates myogenesis by triggering the differentiation activity of pRb. *J Cell Biol.* 2000;151:1295-1304.
- Polager S, Ginsberg D. p53 and E2f: partners in life and death. *Nat Rev Cancer.* 2009;9:738-748.
- Shin DH, Lee HY, Lee HW, et al. In situ localization of p53, bcl-2 and bax mRNAs in rat ocular tissue. *Neuroreport.* 1999;10:2165-2167.
- Tendler Y, Weisinger G, Coleman R, et al. Tissue-specific p53 expression in the nervous system. *Brain Res Mol Brain Res.* 1999;72:40-46.
- Donehower LA, Harvey M, Slagle BL, et al. Mice deficient for p53 are developmentally normal but susceptible to spontaneous tumours. *Nature.* 1992;356:215-221.
- Jacks T, Remington L, Williams BO, et al. Tumor spectrum analysis in p53-mutant mice. *Curr Biol.* 1994;4:1-7.
- Reichel MB, Ali RR, D'Esposito F, et al. High frequency of persistent hyperplastic primary vitreous and cataracts in p53-deficient mice. *Cell Death Differ.* 1998;5:156-162.
- Ikeda S, Hawes NL, Chang B, Avery CS, Smith RS, Nishina PM. Severe ocular abnormalities in C57BL/6 but not in 129/Sv p53-deficient mice. *Invest Ophthalmol Vis Sci.* 1999;40:1874-1878.
- O'Connor JC, Wallace DM, O'Brien CJ, Cotter TG. A novel antioxidant function for the tumor-suppressor gene p53 in the retinal ganglion cell. *Invest Ophthalmol Vis Sci.* 2008;49:4237-4244.
- Miller TJ, Schneider RJ, Miller JA, et al. Photoreceptor cell apoptosis induced by the 2-nitroimidazole radiosensitizer, CI-1010, is mediated by p53-linked activation of caspase-3. *Neurotoxicology.* 2006;27:44-59.
- Borges HL, Linden R. Gamma irradiation leads to two waves of apoptosis in distinct cell populations of the retina of newborn rats. *J Cell Sci.* 1999;112(Pt 23):4315-4324.
- Morgan SE, Kastan MB. p53 and ATM: cell cycle, cell death, and cancer. *Adv Cancer Res.* 1997;71:1-25.
- Borges HL, Chao C, Xu Y, Linden R, Wang JY. Radiation-induced apoptosis in developing mouse retina exhibits dose-dependent requirement for ATM phosphorylation of p53. *Cell Death Differ.* 2004;11:494-502.
- Joo CK, Choi JS, Ko HW, et al. Necrosis and apoptosis after retinal ischemia: involvement of NMDA-mediated excitotoxicity and p53. *Invest Ophthalmol Vis Sci.* 1999;40:713-720.
- Rosenbaum DM, Rosenbaum PS, Gupta H, et al. The role of the p53 protein in the selective vulnerability of the inner retina to transient ischemia. *Invest Ophthalmol Vis Sci.* 1998;39:2132-2139.
- Westlund BS, Cai B, Zhou J, Sparrow JR. Involvement of c-Abl, p53 and the MAP kinase JNK in the cell death program initiated in A2E-laden ARPE-19 cells by exposure to blue light. *Apoptosis.* 2009;14:31-41.
- Lansel N, Hafezi F, Marti A, Hegi M, Reme C, Niemeyer G. The mouse ERG before and after light damage is independent of p53. *Doc Ophthalmol.* 1998;96:311-320.
- Marti A, Hafezi F, Lansel N, et al. Light-induced cell death of retinal photoreceptors in the absence of p53. *Invest Ophthalmol Vis Sci.* 1998;39:846-849.
- Wu J, Trogadis J, Bremner R. Rod and cone degeneration in the rd mouse is p53 independent. *Mol Vis.* 2001;7:101-106.
- Hopp RM, Ransom N, Hilsenbeck SG, Papermaster DS, Windle JJ. Apoptosis in the murine rd1 retinal degeneration is predominantly p53-independent. *Mol Vis.* 1998;4:5.
- Ali RR, Reichel MB, Kanuga N, et al. Absence of p53 delays apoptotic photoreceptor cell death in the rds mouse. *Curr Eye Res.* 1998;17:917-923.
- Laurie NA, Donovan SL, Shih CS, et al. Inactivation of the p53 pathway in retinoblastoma. *Nature.* 2006;444:61-66.
- Vuong L, Conley SM, Al-Ubaidi MR. Expression and role of p53 in the retina. *Invest Ophthalmol Vis Sci.* In press.
- Tan E, Wang Q, Quiambao AB, et al. The relationship between opsin overexpression and photoreceptor degeneration. *Invest Ophthalmol Vis Sci.* 2001;42:589-600.
- Sherry DM, Murray AR, Kanan Y, et al. Lack of protein-tyrosine sulfation disrupts photoreceptor outer segment morphogenesis, retinal function and retinal anatomy. *Eur J Neurosci.* 2010;32:1461-1472.
- Tan E, Ding XQ, Saadi A, Agarwal N, Naash MI, al-Ubaidi MR. Expression of cone-photoreceptor-specific antigens in a cell line derived from retinal tumors in transgenic mice. *Invest Ophthalmol Vis Sci.* 2004;45:764-768.
- Soule HD, Vazquez J, Long A, Albert S, Brennan M. A human cell line from a pleural effusion derived from a breast carcinoma. *J Natl Cancer Inst.* 1973;51:1409-1416.
- Iwamoto A, Masuda M, Yoshikura H. Two NIH3T3 cell lines of different origins circulating in the world. *Jpn J Exp Med.* 1985;55:129-131.
- Marine JC, Lozano G. Mdm2-mediated ubiquitylation: p53 and beyond. *Cell Death Differ.* 2010;17:93-102.
- Young RW. Cell differentiation in the retina of the mouse. *Anat Rec.* 1985;212:199-205.
- Yang A, Kaghad M, Wang Y, et al. p63, a p53 homolog at 3q27-29, encodes multiple products with transactivating, death-inducing, and dominant-negative activities. *Mol Cell.* 1998;2:305-316.
- Jost CA, Marin MC, Kaelin WG Jr. p73 is a simian [correction of human] p53-related protein that can induce apoptosis. *Nature.* 1997;389:191-194.
- Kaghad M, Bonnet H, Yang A, et al. Monoallelically expressed gene related to p53 at 1p36, a region frequently deleted in neuroblastoma and other human cancers. *Cell.* 1997;90:809-819.

40. Melino G. p73, the "assistant" guardian of the genome? *Ann N Y Acad Sci.* 2003;1010:9-15.
41. Mills AA, Zheng B, Wang XJ, Vogel H, Roop DR, Bradley A. p63 is a p53 homologue required for limb and epidermal morphogenesis. *Nature.* 1999;398:708-713.
42. Yang A, Schweitzer R, Sun D, et al. p63 is essential for regenerative proliferation in limb, craniofacial and epithelial development. *Nature.* 1999;398:714-718.
43. Yang A, Walker N, Bronson R, et al. p73-deficient mice have neurological, pheromonal and inflammatory defects but lack spontaneous tumours. *Nature.* 2000;404:99-103.
44. Ekholm SV, Reed SI. Regulation of G(1) cyclin-dependent kinases in the mammalian cell cycle. *Curr Opin Cell Biol.* 2000;12:676-684.
45. Kong Y, Cui H, Ramkumar C, Zhang H. Regulation of senescence in cancer and aging. *J Aging Res.* 2011;2011: 963172.
46. Soria G, Speroni J, Podhajcer OL, Prives C, Gottifredi V. p21 differentially regulates DNA replication and DNA-repair-associated processes after UV irradiation. *J Cell Sci.* 2008;121: 3271-3282.
47. Chen J, Jackson PK, Kirschner MW, Dutta A. Separate domains of p21 involved in the inhibition of Cdk kinase and PCNA. *Nature.* 1995;374:386-388.
48. Al-Ubaidi MR, Mangini NJ, Quiambao AB, et al. Unscheduled DNA replication precedes apoptosis of photoreceptors expressing SV40 T antigen. *Exp Eye Res.* 1997;64:573-585.
49. Donovan SL, Schweers B, Martins R, Johnson D, Dyer MA. Compensation by tumor suppressor genes during retinal development in mice and humans. *BMC Biol.* 2006;4:14.
50. Kapic A, Helmbold H, Reimer R, Klotzsche O, Deppert W, Bohn W. Cooperation between p53 and p130(Rb2) in induction of cellular senescence. *Cell Death Differ.* 2006;13: 324-334.
51. Harbour JW, Dean DC. The Rb/E2F pathway: expanding roles and emerging paradigms. *Genes Dev.* 2000;14:2393-2409.
52. Sun A, Bagella L, Tutton S, Romano G, Giordano A. From G0 to S phase: a view of the roles played by the retinoblastoma (Rb) family members in the Rb-E2F pathway. *J Cell Biochem.* 2007; 102:1400-1404.
53. Helin K, Wu CL, Fattaey AR, et al. Heterodimerization of the transcription factors E2F-1 and DP-1 leads to cooperative transactivation. *Genes Dev.* 1993;7:1850-1861.
54. Flemington EK, Speck SH, Kaelin WG Jr. E2F-1-mediated transactivation is inhibited by complex formation with the retinoblastoma susceptibility gene product. *Proc Natl Acad Sci U S A.* 1993;90:6914-6918.
55. Graziano V, De L. V. Role of p63 in cancer development. *Biochim Biophys Acta.* 2011;1816:57-66.
56. Sidle A, Palaty C, Dirks P, et al. Activity of the retinoblastoma family proteins, pRB, p107, and p130, during cellular proliferation and differentiation. *Crit Rev Biochem Mol Biol.* 1996;31:237-271.